Published in final edited form as:
Biochem Pharmacol. 2013 April 15; 85(8): 1057–1065. doi:10.1016/j.bcp.2013.01.015.

Tamoxifen magnifies therapeutic impact of ceramide in human colorectal cancer cells independent of p53*

Samy A.F. Morad[1,+], **James P. Madigan**[2,‡], **Jonathan C. Levin**[1], **Noha Abdelmageed**[1], **Ramin Karimi**[1], **Daniel W. Rosenberg**[2], **Mark Kester**[3], **Sriram S. Shanmugavelandy**[3], and **Myles C. Cabot**[1]

[1]John Wayne Cancer Institute, Santa Monica, California, USA

[2]Center for Molecular Medicine, University of Connecticut Health Center, Farmington, Connecticut

[3]Department of Pharmacology, Pennsylvania State University, Hershey, Pennsylvania

Abstract

Poor prognosis in patients with later stage colorectal cancer (CRC) necessitates the search for new treatment strategies. Ceramide, because of its role in orchestrating death cascades in cancer cells, is a versatile alternative. Ceramide can be generated by exposure to chemotherapy or ionizing radiation, or it can be administered in the form of short-chain analogs (C6-ceramide). Because intracellular P-glycoprotein (P-gp) plays a role in catalyzing the conversion of ceramide to higher sphingolipids, we hypothesized that administration of P-gp antagonists with C6-ceramide would magnify cell death cascades. Human CRC cell lines were employed, HCT-15, HT-29, and LoVo. The addition of either tamoxifen, VX-710, verapamil, or cyclosporin A, antagonists of P-gp, enhanced C6-ceramide cytotoxicity in all cell lines. In depth studies with C6-ceramide and tamoxifen in LoVo cells showed the regimen induced PARP cleavage, caspase-dependent apoptosis, mitochondrial membrane permeabilization (MMP), and cell cycle arrest at G1 and G2. At the molecular level, the regimen, but not single agents, induced time-dependent upregulation of tumor suppressor protein p53; however, introduction of a p53 inhibitor staved neither MMP nor apoptosis. Nanoliposomal formulations of C6-ceramide and tamoxifen were also effective, yielding synergistic cell kill. We conclude that tamoxifen is a favorable adjuvant for enhancing

*This work was presented in part at the ASBMB 2012 Experimental Biology Meeting, April 21–25, San Diego, CA. Drs. Morad and Madigan contributed equally to this research.

Correspondence to: Myles C. Cabot, Department of Experimental Therapeutics, John Wayne Cancer Institute at Saint John's Health Center, 2200 Santa Monica Blvd, Santa Monica, CA 90404, USA. cabot@jwci.org. Phone: (310) 998-3924. Fax: (310) 582-7325.
+Affiliated with Department of Pharmacology, South Valley University, Qena, Egypt.
‡Current address: Laboratory of Cell Biology, NCI, Bethesda, MD

Competing interests

The Penn State Research Foundation has licensed ceramide nanoliposomes and other nanoliposomal technology to Keystone Nano Inc (State College, PA). MK is the Chief Medical Officer of Keystone Nano Inc.

Authors' contribution

Samy A.F. Morad, James P. Madigan, Jonathan C. Levin, Noha Abdelmageed, Ramin Karimi, Daniel W. Rosenberg, and Myles C. Cabot contributed fundamentally to the acquisition and interpretation of data. Sriram S. Shanmugavelandy and Mark Kester formulated, evaluated, and provided nanoliposomal preparations. Myles C. Cabot, Samy A.F. Morad, and Jonathan C. Levin contributed to writing and compiling the manuscript, and all authors read, evaluated, interpreted, and approved the manuscript and extant data. Experiments were conceived and designed by all authors.

C6-ceramide cytotoxicity in CRC, and demonstrates uniquely integrated effects. The high frequency of expression of P-gp in CRC presents an adventitious target for complementing ceramide-based therapies, a strategy that could hold promise for treatment of resistant disease.

Keywords

colorectal cancer; ceramide; C6-ceramide; tamoxifen; P-glycoprotein; p53

1. Introduction

Colorectal cancer (CRC) is the third most common cancer in both men and women; in 2012 an estimated 51,690 deaths are predicted. Surgical removal may be curative for colorectal cancers that have not spread; however, cure is not possible for most patients with metastatic disease. Conventional and targeted chemotherapies are available for these patients. For example, orally active capecitabine (Xeloda®), Oxaplatin (Eloxatin®), and Irinotecan (Camptosar®) work as most anticancer agents, by interfering with the ability of rapidly growing cancer cells to divide, whereas targeted agents like Bevacizumab (Avastin®) and Cetuximab (Erbitux®) are monoclonal antibodies that bind to vascular endothelial growth factor, hindering development of tumor blood supply and blocking the epidermal growth factor receptor, respectively. Conventional and targeted agents are often used in combination in chemotherapy-naïve patients with newly diagnosed metastatic disease. When colorectal cancers are detected early, the 5-year survival is 91%. However, only approximately 39% of patients are diagnosed with localized disease. Poor prognosis in patients with later stage diseases necessitates the search for new treatment strategies.

Cancer cell response to chemotherapy is often associated with induction of apoptosis, and resistance to apoptosis often accompanies tumor progression [1]. The reinstatement of apoptotic pathways in tumor cells that have acquired blocks is a promising area of investigation [2]. Of the many signaling molecules at work, it is now well known that a number of cell death cascades engage the sphingolipid ceramide as intracellular orchestrator [3]. Ceramide can be generated in mass in response to stressors such as radiation and chemotherapy [4–7]. Once generated, either through a *de novo* pathway or by sphingomyelin hydrolysis, intracellular conversion of ceramide to a variety of metabolites is key in regulating apoptotic versus mitogenic downstream events [8–10]. For example, hydrolysis by ceramidase and glycosylation by glucosylceramide synthase (GCS) limit ceramide potency, and in the case of the former, contribute to generation of mitogenic sphingolipids [11–13].

A number of studies demonstrate that modulation of ceramide metabolism is an effective means for increasing sensitivity to anticancer agents [5, 7, 10, 14, 15]. Whereas GCS and acid ceramidase have been investigated as prime targets, our group was the first to demonstrate that antagonists of the multidrug transporter protein, P-glycoprotein (P-gp) (gene symbol ABCB1), inhibit conversion of ceramide to glucosylceramide (GC) in multidrug resistant cancer cells [16]. Thus, multidrug transporters like P-gp present an alternative to GCS for regulation of ceramide metabolism and possibly for regulation of ceramide potency.

The present study focuses on short-chain ceramides, analogs of natural long-chain ceramides and candidates for clinical investigation [17, 18]. Agents like C6-ceramide can be used in place of ceramide-generating drugs [6, 7, 19], and whereas metabolism can be controlled in much the same manner [20–22], short-chain ceramides offer the advantage of nanoliposomal formulation, including combinatorial formulations [17]. Here we demonstrate, in several

human CRC cell lines, that C6-ceramide cytotoxicity can be magnified by a variety of P-gp antagonists such as tamoxifen, cyclosporin A, VX-710 (biricodar), and verapamil [23]. Cytotoxic response to C6-ceramide-P-gp antagonist combinations was accompanied by caspase activation, poly ADP ribose polymerase (PARP) cleavage, DNA fragmentation, cell cycle arrest, increased mitochondrial membrane permeability (MMP), and enhanced protein expression of tumor suppressor p53.

Increased expression of multidrug resistance proteins occurs early in colorectal carcinogenesis [24], and these proteins are often constituents of colorectal cancer cells regardless of chemotherapy history. The high frequency of expression of drug transporter proteins in CRC presents a novel target for enhancing ceramide-based therapies, a strategy that could hold promise for patients with local and distant metastatic disease.

2. Materials and methods

2.1 Cell culture

Three CRC lines were used, LoVo, HT-29, and HCT-15. All were obtained from the American Type Culture Collection (Manassas, VA) and propagated in RPMI-1640 medium (Invitrogen Corp, Carlsbad, CA) containing 10% fetal bovine serum (FBS) (HyClone, Logan, UT, and Atlanta Biological, Atlanta, GA), 50 units/ml penicillin, 50 μg/ml streptomycin, and 584 mg/L L-glutamine (Invitrogen Corp, Carlsbad, CA). The cell lines were expanded and cryopreserved in liquid nitrogen in the investigator's laboratory. The cell lines were not tested or authenticated over and above documentation provided by the ATCC, which included antigen expression, DNA profile, and cytogenic analysis. Cells were grown in humidified conditions in a tissue culture incubator with 95% air and 5% CO_2, at 37 °C. Confluent cells were subcultured using Gibco 0.05% trypsin/0.53 mM EDTA solution (Invitrogen Corp, Carlsbad, CA). N-hexanoyl[1-^{14}C]-D-*erythro*-sphingosine (C6-ceramide) (55 mCi/mmol) was from American Radiolabeled Chemicals (St. Louis, MO). Pifithrin-α, a p53 inhibitor, was from Cayman Chemical (Ann Arbor, MI). Pan-caspase inhibitor, Z-VAD-FMK, from BD Pharmigen (San Diego), was solubilized in ethanol and stored as a 40 mM stock at −20°C.

2.2 Cell viability assays

Cells were seeded in 96-well plates. LoVo and HT-29 cells were seeded at 10,000 cells/well, and HCT-15 cells were seeded at 5,000 cells/well. Cells were seeded in 0.1 ml complete medium and allowed to attach at 37°C for 24 h before adding drugs. Verapamil-HCl, cyclosporin A, tamoxifen-HCl, and *N*-desmethyltamoxifen-HCl were purchased from Sigma Chemical Co, St. Louis, MO. C6-Ceramide (*N*-hexanoyl-D-*erthyro*-sphingosine) was purchased from Avanti Polar Lipids, Alabaster, AL. VX-710 (biricodar) was a gift from Vertex Pharmaceuticals, Cambridge, MA. All drugs, except VX-710, were dissolved in 100% ethanol and stored as stock solutions (10 mM) at −20 °C. VX-710 was dissolved in dimethyl sulfoxide at a concentration of 10 mM and stored at −20 °C. Drugs were diluted freshly into culture medium containing 1% FBS and added to wells to a total volume of 0.2 ml, thus the final concentration of FBS during treatment was 5.5%. After addition of agents, cells were incubated at 37 °C for 72 or 96 hr, and cell viability was determined using CellTiter 96 Aqueous One Solution cell proliferation assay kit, Promega, Milwaukee, WI. A Microplate Fluorescent Reader FL600, BIO-TEK Instruments (Winooski, VT) was used to record absorbance at 490 nm.

2.3 Caspace-Glo® 3/7 assay

Cells were seeded in 96-well plates in 50 μl complete medium, and grown at 37 °C for 24 h. Agents were then added to a final volume of 0.1 ml/well, and cells were incubated for an

additional 24 h at 37°C and then treated with Caspace-Glo® 3/7 Assay mixture (Promega, Milwaukee, WI). Plates were covered and incubated at room temperature for 1–2 h. Results were evaluated using the Glomax Multi Detection System (Promega, Milwaukee, WI), following the luminescence protocol supplied.

2.4 Western blotting, PARP cleavage, caspase-3 assay

Primary antibody detecting β-tubulin (clone TUB 2.1, catalog # T4026) was from Sigma-Aldrich, St. Louis, MO. PARP, cleaved PARP (catalog # 9542), caspase-3 (catalog # 9662), p53 (clone 7F5, catalog # 2527), and GAPDH (clone 14C10, catalog # 2118) were from Cell Signaling Technology, Danvers, MA. LoVo cells were seeded in 6-cm dishes (5×10^5) 24 h prior to treatment. Cells were then given fresh medium, and floating cells were removed. Cells were treated for 24 h with C6-ceramide, tamoxifen, or combinations thereof, and controls were treated with ethanol vehicle. After treatment, floating cells were collected and attached cells were trypsinized and centrifuged together with the floating population. Cell pellets were lysed in NP-40 lysis buffer [50 mM Tris/HCl, pH 7.4, 150 mM NaCl and 1% Nonidet P40, supplemented with Complete Protease Inhibitor Cocktail tablets and PhosStop phosphatase inhibitors (Roche, Indianapolis, Indiana) along with 0.5 mM PMSF] and centrifuged to remove insoluble material. Protein (40 μg), boiled in 2X Laemmli sample buffer, was then resolved on SDS/PAGE (12 or 15% gels) and transferred onto Immobilon PVDF membrane. The membrane was blocked for 1 h at room temperature in blocking buffer containing 5% (w/v) non-fat dried skimmed milk in TBS-Tween 20 (TBST) (20 mM Tris/HCl, pH 7.6, 137 mM NaCl, 0.2% Tween 20). Membranes were probed overnight with appropriate primary antibodies in blocking buffer. After extensive washing in TBST buffer, blots were probed with either anti-rabbit or anti-mouse IgG-horseradish peroxidase (HRP)-conjugated secondary antibodies (Cell Signaling Technology, Danvers, MA) in blocking buffer for 30 min. After extensive washing in TBST, membranes were incubated in Immobilon Western Blot Chemiluminescent HRP Substrate (Millipore) and the signals developed on biomax XAR film (Kodak).

2.5 DNA fragmentation and cell cycle analyses

Progression of cells through cell cycle and DNA fragmentation were examined using flow cytometry. DNA content was measured according to published protocol [25] with modification. Cells were seeded in 6-cm dishes at 200,000 cells/dish in 10% FBS medium. The following day the medium was removed, and cells were treated with indicated agents in fresh medium containing 2.5% FBS for 24 h. Cells were collected by trypsinization then washed with cold PBS and fixed in 70% ethanol. DNA was stained for 4 h in the dark with 0.5 ml hypotonic propidium iodide buffer (0.1% sodium citrate, 50 μg/mL DNase-free RNase A, 0.1% Triton X-100). DNA content was analyzed using a FACScan, and cell cycle analysis and sub G0 (apoptosis marker) were assessed using FCS Express 4 (De Novo Software).

2.6 Mitochondrial membrane permeabilization

MMP was measured using JC-1 (Cell Technology, Mountain View, CA) to gauge changes in mitochondrial membrane potential via depolarization. CRC cells were plated as in the DNA fragmentation experiments and treated the following day with agents for 18 h. JC-1 is a radiometric dye that exists as a monomer in the cytosol (green) and also accumulates as aggregates in the mitochondria which stain red. Quantitative analysis of MMP was detected by JC-1 at FL-1 (green) and FL-2 (red) using flow cytometry.

2.7 Cellular metabolism of C6-ceramide

LoVo cells were seeded into 6-well plates (300,000/well) in medium containing 5% FBS. The following day cells were pretreated in the absence or presence of tamoxifen (5.0 μM, ethanol vehicle) for 1 h after which [^{14}C]C6-ceramide was added (20 μM) using ethanol vehicle. After a 24 h incubation, total cellular lipids were extracted from PBS-washed monolayers [26] and analyzed by thin-layer chromatography (TLC) and liquid scintillation counting (LSC) as described previously [20]. A versatile solvent system for separation of C6-ceramide, C6-GC, C6-lactosylceramide (LC), and C6-sphingomyelin (SM) consisted of chloroform/methanol/acetic acid/water (65:25:2:2, v/v) in filter paper-lined chromatography tanks. Commercial lipid standards were co-chromatographed (Avanti Polar Lipids, Alabaster, AL; Matreya, Pleasant Gap, PA).

2.8 Nanoliposomal formulation

Pegylated nanoliposomes were prepared as described in earlier studies [17, 27]. Preparations were stable at room temperature for 1–2 months.

2.9 Statistical analysis

The results are expressed as the mean ± S.E. (standard error) and were analyzed by ANOVA. Differences among treatment groups were assessed by Tukey's test. Differences were considered significant at $P \leq 0.05$. An asterisk (*) used in specific figures, denotes significance; figure legends also provide comments on statistical significance.

3. Results

3.1 Tamoxifen enhances C6-ceramide cytotoxicity in CRC cells

Earlier we reported that antagonists of P-gp inhibit ceramide metabolism in multidrug resistant cancer cells at the step of glycosylation, a finding that posed the possibility of employing P-gp antagonists to intensify the 'ceramide effect.' Of the agents assessed, tamoxifen was shown to be the most potent inhibitor of GC synthesis in human ovarian cancer cells, NCI/ADR-RES, formerly designated MCF-7/AdrR. Because P-gp expression correlates with pathological grading of CRC, being highly expressed in well differentiated tumors [28], we focused our study on CRC and initiated work using tamoxifen as lead compound. Figure 1A shows that the CRC cell line, LoVo, was relatively refractory to C6-ceramide exposure, with viability maintained at 80% of control at 5 μM, after a 72 h exposure. However, the inclusion of tamoxifen, which alone decreased viability to 86% of control, produced 18% viability (Fig. 1B). Combination C6-ceramide-tamoxifen was also effective in other CRC cell lines, although the effect was more additive (Fig. 1C, D). The data in Table 1 show that glycosylation was the principle route of C6-ceramide metabolism in LoVo cells. C6-GC accounted for 82.3 and 58.9% of total cellular ^{14}C in cells in the absence and presence of tamoxifen, respectively. Tamoxifen exposure doubled the amount of free intracellular C6-ceramide. Interestingly, we believe in order to compensate for the decrease in C6-GC synthesis and the increase in free C6-ceramide when tamoxifen was present, LoVo cells increased the amount of C6-SM synthesized by 2.6-fold. It should be noted that these results are exclusive of hydrolysis, a route that could not be evaluated using [1-^{14}C]C6-ceramide. Cells were exposed to 20 μM C6-ceramide in an effort to improve uptake and drive metabolic routing.

3.2 Representative P-gp antagonists enhance C6-ceramide cytotoxicity in LoVo cells and alter C6-ceramide metabolism

Whereas one significant off-target effect of tamoxifen is P-gp antagonism [29], we next sought to determine whether other P-gp-interacting agents would enhance C6-ceramide

cytotoxicity. As shown in Fig. 2A, verapamil and cyclosporine A, first-generation modulators, and VX-710, a third generation P-gp modulator, were effective enhancers of C6-ceramide response in LoVo cells. Verapamil and VX-710 demonstrated weak cytotoxicity alone; however, when administered with C6-ceramide, which was only moderately cytotoxic, viability fell precipitously (Fig. 2A, cross-hatch). The data in Fig. 2B demonstrate that *N*-desmethyltamoxifen, the major *in vivo* metabolite of tamoxifen in humans, was also effective in combination with C6-ceramide, as shown in side-by-side comparisons with tamoxifen. In addition, Fig. 2B shows that the effect of tamoxifen on C6-ceramide cytotoxicity was dose-dependent, being more effective at 10 than at 5 μM (compare cross-hatch data). These results clearly show that P-gp antagonists enhance the cytotoxic activity of C6-ceramide in human CRC cells, and in LoVo cells we demonstrate that tamoxifen modifies C6-ceramide metabolism (see Table 1).

3.3 C6-ceramide and tamoxifen promote hallmark apoptotic responses and block cell cycle in LoVo cells

We next endeavored to identify the type of cell death elicited by combination C6-ceramide-tamoxifen. As shown in Fig. 3, drug consolidation produced strong activation of caspase 3/7 in LoVo, HCT-15, and HT-29 cells. For example, in HT-29 cells C6-ceramide, tamoxifen, and the combination produced an approximate 1.5-, 1.5-, and 5-fold increase in caspase 3/7 activation. The data in Fig. 3B demonstrate the effects of single agent versus combination treatment on other hallmarks of apoptosis. It is noteworthy that neither single agent tamoxifen nor C6-ceramide elicited production of the active, cleaved form of effector caspase 3; however, drug co-administration was markedly effective in caspase 3 activation. This response followed suit with PARP cleavage, and yielded a robust increase with combination C6-ceramide-tamoxifen (Fig. 3B). DNA fragmentation, another feature of programmed cell death, likewise occurred only in response to the drug duo as opposed to the single agents (Fig. 3C). Apoptosis (DNA fragmentation) was reversed *in toto* by inclusion of a pan-caspase inhibitor (Fig. 3C), demonstrating that C6-ceramide-tamoxifen induce caspase-dependent cell death. In addition to apoptotsis, C6-ceramide-tamoxifen promoted cell cycle arrest at both G1 and G2 (Fig. 4), tumor cell growth and division phases.

3.4 Combination C6-ceramide-tamoxifen upregulate p53 expression and induce mitochondrial depolarization in LoVo cells

p53 is a tumor suppressor in many cancers, and expression induces growth arrest or apoptosis, depending on the physiological circumstances and cell type. p53 activation has been shown to induce mitochondrial signaling by binding to BCL2 [30]. In colorectal cancer, activation of p53 is associated with induction of apoptosis [31–33]. In order to elucidate molecular responses to C6-ceramide-tamoxifen, we studied the effect of this drug combination on p53 expression. As shown in Fig. 5A, C6-ceramide-tamoxifen upregulated p53 expression in a time-dependent fashion, with initial increases noted by 12 h. The influence of single agents versus combination on p53 expression is shown in Fig. 5B. Whereas tamoxifen at 5 and 10 μM had little effect on expression and single agent C6-ceramide (5 μM) displayed moderate impact, the combination was clearly a strong inducer of p53 expression. Ceramide can induce MMP [3], a key event in apoptotic signaling. The data in Fig. 4C demonstrate that C6-ceramide-tamoxifen enhances MMP in LoVo cells, as reflected by the >30% increase in mitochondrial depolarization ($\Delta\psi m$), compared with 10% in control. Inactivation of p53 by inclusion of pifithrin-α that blocks p53-dependent transcriptional activation and apoptosis, failed to diminish C6-ceramide-tamoxifen-enhanced MMP (Fig. 5C). Inactivation of p53 also failed to reverse apoptosis (DNA fragmentation) caused by C6-ceramide-tamoxifen (Fig. 5D). These results suggest that p53 activation is not an essential element in the apoptotic response to C6-ceramide-tamoxifen exposure in CRC cells.

3.5 Nanoliposomal formulations of C6-ceramide and tamoxifen are synergistic for LoVo cell kill

Kester and colleagues have demonstrated that nanoliposomal formulations of C6-ceramide improve delivery and systemic retention, *in vivo* [34]. With future *in vivo* studies in mind, we sought to establish whether nanoliposomal formulations of C6-ceramide and tamoxifen would be efficacious in *in vitro* systems. Two reagents were formulated for this work, nanoliposomal tamoxifen and a composite nanoliposome that contains both C6-ceramide and tamoxifen in the same particle, which is to say that the C6-ceramide nanoliposomes serve as the vehicle for tamoxifen. The data in Fig. 6A demonstrate that whereas low-dose nanoliposomal tamoxifen (5 μM) imparted no cytotoxicity and low-dose nanoliposomal C6-ceramide (5 μM) was only slightly cytotoxic (78% viability), the combination reduced cell viability to 34% of control, a response that was synergistic with a CI (combination index) of 0.37, as noted in the figure. In addition, exposure to composite nanoliposomes yielded higher cytotoxicity than did mixing of individual nanoliposomes. Therefore, composite nanoliposomes could comprise a promising platform for delivery of this apoptosis-inducing drug regimen. *N*-desmethyltamoxifen, the major *in vivo* tamoxifen metabolite in humans, was also effective when administered in combination with nanoliposomal C6-ceramide (Fig. 6B). For example, whereas nanoliposomal C6-ceramide (5 μM) reduced viability to only 80% of control and *N*-desmethyltamoxifen (5 μM) was essentially without influence, the combination brought viability to 45% of control.

4. Discussion

Tamoxifen has been the subject of several investigations in CRC; however, few studies have enlisted tamoxifen as an adjuvant with ceramide in this neoplasm. In *in vivo* experiments, Shen et al [35] demonstrated that tamoxifen reversed multidrug resistance in CRC in nude mice, independent of estrogen receptor expression, and a forerunner study showed that tamoxifen circumvented doxorubicin resistance in freshly isolated human gastrointestinal cells [36]. These actions likely occur via antagonism of P-gp, because tamoxifen directly binds and inhibits P-gp [29, 37]. Other works have also demonstrated growth-inhibitory effects of tamoxifen in CRC [38–40]. Thus, tamoxifen has a myriad of interesting, beneficial effects in colon cancer.

Whereas tamoxifen at the concentrations we employed was only mildly cytotoxic, the addition of a cell-deliverable ceramide, C6-ceramide, resulted in magnified cytotoxic responses. Other more representative P-gp antagonists, in combination with C6-ceramide, produced similar cytotoxic endpoints, and we have previously demonstrated that these agents as well block GC production in cultured multidrug resistant cancer cells [16]. Therefore, one plausible explanation for the enhanced effect is that P-gp antagonists extend the intracellular residence time of C6-ceramide, an action that would perpetuate ceramide signaling. Because LoVo cells convert C6-ceramide to higher sphingolipids (see Table 1), preserving intracellular levels of C6-ceramide could be a contributing factor underlying the intensified cytotoxicity of this drug combination; however, as discussed below, maintaining high levels of C6-ceramide might not be an essential element in eliciting response.

Our work demonstrates that cell death was via caspase-dependent apoptosis. It is noteworthy that neither C6-ceramide nor tamoxifen caused DNA fragmentation (see Fig. 3C, bar graph), whereas the combination produced both supra-additive DNA fragmentation and caspase-3 activation and subsequent PARP cleavage. It is well known that natural ceramides activate pro-apoptotic events; the same has been demonstrated with short-chain ceramides [41–43]. Interestingly, in a model of human keratinocytes, C6-ceramide exposure induced apoptosis via the salvage pathway [44], wherein C6-ceramide is hydrolyzed by ceramidase, and the liberated sphingosine reacylated by ceramide synthase to generate long-chain ceramides. We

have previously shown that tamoxifen enhances the formation of long-chain ceramide from C6-ceramide in LoVo cells [20]. Whereas ceramidase and the salvage pathway can diminish the potency of short-chain ceramides, this biochemistry can be a double-edged sword producing specific apoptosis-inducing molecular species of long-chain ceramides and also yield sphingosine for synthesis of sphingosine 1-phosphate, a mitogenic entity. The extent to which long-chain ceramides generated in response to C6-ceramide-tamoxifen treatment in LoVo cells contribute to cytotoxicity is a subject of our ongoing work.

Tamoxifen can affect apoptosis via the mitochondrial pathway [38, 39], and both tamoxifen and ceramide can exact downstream antiproliferative response through multiple cascades [39, 45]. In our studies herein, we propose that C6-ceramide and tamoxifen act independently as well as in concert to elicit signaling events culminating in cell cycle arrest and apoptosis. In this context, only the combination increased the expression of p53 (see Fig. 5), a regulator of cell cycle that functions as a tumor sensor in cancer. Interestingly, previous studies have shown that restoration of p53 is essential and sufficient for the induction of apoptosis in CRC [31–33]. In our study we show that the drug duo induces apoptosis and MMP independent of p53 upregulation and independent of p53 status, because LoVo, HCT-15, and HT-29 cells are p53 wild-type, p53 mutant, and p53 mutant, respectively.

C6-ceramide in nanoliposomal form has been shown effective *in vitro* and *in vivo* [17, 34, 45–47]. In the present work, we have formulated a composite platform that uses C6-ceramide nanoliposomes as the vehicle for tamoxifen and shown this course to be equal or superior to co-administration of single agent C6-ceramide and tamoxifen nanoliposomes.

5. Conclusions

Taken together, we propose that combination C6-ceramide-tamoxifen, which we show elicits aggressive apoptotic responses, comprises a promising, innovative treatment strategy in CRC. This drug duo demonstrates uniquely orchestrated effects. Fittingly, there is an extensive literature on tamoxifen in colon cancer; however, the present work illustrates a new aspect of tamoxifen potential. In addition, the use of P-gp antagonists to direct ceramide metabolism ought be considered as a means to enhance ceramide-orchestrated events for the induction of cancer cell death.

Acknowledgments

National Institutes of General Medical Science (grant no. GM77391, to MCC).

Abbreviation

CRC	colorectal cancer
P-gp	P-glycoprotein
GCS	glucosylceramide synthase
GC	glucosylceramide
PARP	poly ADP ribose polymerase
MMP	mitochondrial membrane permeabilization
FBS	fetal bovine serum
ATCC	American Type Culture Collection

HRP	IgG-horseradish peroxidase
TLC	thin layer chromatography
LSC	liquid scintillation counting
LC	C6-lactosylceramide
SM	C6-sphingomyelin
Δψm	mitochondrial depolarization
C6-GC	C6-glucosylceramide
C6-SM	C6-sphingomyelin

References

1. Naik P, Karrim J, Hanahan D. The rise and fall of apoptosis during multistage tumorigenesis: down-modulation contributes to tumor progression from angiogenic progenitors. Genes Dev. 1996; 10:2105–16. [PubMed: 8804306]
2. Wang CY, Cusack JC Jr, Liu R, Baldwin AS Jr. Control of inducible chemoresistance: enhanced anti-tumor therapy through increased apoptosis by inhibition of NF-kappaB. Nat Med. 1999; 5:412–7. [PubMed: 10202930]
3. Morad SA, Cabot MC. Ceramide-orchestrated signalling in cancer cells. Nat Rev Cancer. 2013; 13:51–65. [PubMed: 23235911]
4. Kolesnick R, Fuks Z. Radiation and ceramide-induced apoptosis. Oncogene. 2003; 22:5897–906. [PubMed: 12947396]
5. Reynolds CP, Maurer BJ, Kolesnick RN. Ceramide synthesis and metabolism as a target for cancer therapy. Cancer Lett. 2004; 206:169–80. [PubMed: 15013522]
6. Charles AG, Han TY, Liu YY, Hansen N, Giuliano AE, Cabot MC. Taxol-induced ceramide generation and apoptosis in human breast cancer cells. Cancer Chemother Pharmacol. 2001; 47:444–50. [PubMed: 11391861]
7. Maurer BJ, Melton L, Billups C, Cabot MC, Reynolds CP. Synergistic cytotoxicity in solid tumor cell lines between N-(4-hydroxyphenyl)retinamide and modulators of ceramide metabolism. J Natl Cancer Inst. 2000; 92:1897–909. [PubMed: 11106681]
8. Merrill AH Jr, Schmelz EM, Dillehay DL, Spiegel S, Shayman JA, Schroeder JJ, et al. Sphingolipids--the enigmatic lipid class: biochemistry, physiology, and pathophysiology. Toxicol Appl Pharmacol. 1997; 142:208–25. [PubMed: 9007051]
9. Hannun YA, Luberto C, Argraves KM. Enzymes of sphingolipid metabolism: from modular to integrative signaling. Biochemistry. 2001; 40:4893–903. [PubMed: 11305904]
10. Cabot, M. Ceramide Glycosylation and Chemotherapy Resistance. In: Futerman, A., editor. Ceramide Signaling. Georgetown, Texas: Landes Bioscience; 2002. p. 133-9.
11. Zeidan YH, Jenkins RW, Korman JB, Liu X, Obeid LM, Norris JS, et al. Molecular targeting of acid ceramidase: implications to cancer therapy. Curr Drug Targets. 2008; 9:653–61. [PubMed: 18691012]
12. Liu X, Cheng JC, Turner LS, Elojeimy S, Beckham TH, Bielawska A, et al. Acid ceramidase upregulation in prostate cancer: role in tumor development and implications for therapy. Expert Opin Ther Targets. 2009; 13:1449–58. [PubMed: 19874262]
13. Bleicher RJ, Cabot MC. Glucosylceramide synthase and apoptosis. Biochim Biophys Acta. 2002; 1585:172–8. [PubMed: 12531551]
14. Radin NS. Killing tumours by ceramide-induced apoptosis: a critique of available drugs. Biochem J. 2003; 371:243–56. [PubMed: 12558497]
15. Senchenkov A, Litvak DA, Cabot MC. Targeting ceramide metabolism--a strategy for overcoming drug resistance. J Natl Cancer Inst. 2001; 93:347–57. [PubMed: 11238696]

16. Lavie Y, Cao H, Volner A, Lucci A, Han TY, Geffen V, et al. Agents that reverse multidrug resistance, tamoxifen, verapamil, and cyclosporin A, block glycosphingolipid metabolism by inhibiting ceramide glycosylation in human cancer cells. J Biol Chem. 1997; 272:1682–7. [PubMed: 8999846]
17. Tran MA, Smith CD, Kester M, Robertson GP. Combining nanoliposomal ceramide with sorafenib synergistically inhibits melanoma and breast cancer cell survival to decrease tumor development. Clin Cancer Res. 2008; 14:3571–81. [PubMed: 18519791]
18. Stover TC, Kim YS, Lowe TL, Kester M. Thermoresponsive and biodegradable linear-dendritic nanoparticles for targeted and sustained release of a pro-apoptotic drug. Biomaterials. 2008; 29:359–69. [PubMed: 17964645]
19. Perry DK, Carton J, Shah AK, Meredith F, Uhlinger DJ, Hannun YA. Serine palmitoyltransferase regulates de novo ceramide generation during etoposide-induced apoptosis. J Biol Chem. 2000; 275:9078–84. [PubMed: 10722759]
20. Chapman JV, Gouaze-Andersson V, Messner MC, Flowers M, Karimi R, Kester M, et al. Metabolism of short-chain ceramide by human cancer cells--implications for therapeutic approaches. Biochem Pharmacol. 2010; 80:308–15. [PubMed: 20385104]
21. Abe A, Wu D, Shayman JA, Radin NS. Metabolic effects of short-chain ceramide and glucosylceramide on sphingolipids and protein kinase C. Eur J Biochem. 1992; 210:765–73. [PubMed: 1483461]
22. Chan SY, Hilchie AL, Brown MG, Anderson R, Hoskin DW. Apoptosis induced by intracellular ceramide accumulation in MDA-MB-435 breast carcinoma cells is dependent on the generation of reactive oxygen species. Exp Mol Pathol. 2007; 82:1–11. [PubMed: 16624283]
23. Tan B, Piwnica-Worms D, Ratner L. Multidrug resistance transporters and modulation. Curr Opin Oncol. 2000; 12:450–8. [PubMed: 10975553]
24. Meijer GA, Schroeijers AB, Flens MJ, Meuwissen SG, van der Valk P, Baak JP, et al. Increased expression of multidrug resistance related proteins Pgp, MRP1, and LRP/MVP occurs early in colorectal carcinogenesis. J Clin Pathol. 1999; 52:450–4. [PubMed: 10562814]
25. Morad SA, Schmidt C, Buchele B, Schneider B, Wenzler M, Syrovets T, et al. (8R)-3beta,8-dihydroxypolypoda-13E,17E,21-triene induces cell cycle arrest and apoptosis in treatment-resistant prostate cancer cells. J Nat Prod. 2011; 74:1731–6. [PubMed: 21800858]
26. Bligh EG, Dyer WJ. A rapid method of total lipid extraction and purification. Can J Biochem Physiol. 1959; 37:911–7. [PubMed: 13671378]
27. Morad SA, Levin JC, Shanmugavelandy SS, Kester M, Fabrias G, Bedia C, et al. Ceramide-antiestrogen nanoliposomal combinations--novel impact of hormonal therapy in hormone-insensitive breast cancer. Mol Cancer Ther. 11:2352–61. [PubMed: 22962326]
28. Potocnik U, Ravnik-Glavac M, Golouh R, Glavac D. Naturally occurring mutations and functional polymorphisms in multidrug resistance 1 gene: correlation with microsatellite instability and lymphoid infiltration in colorectal cancers. J Med Genet. 2002; 39:340–6. [PubMed: 12011154]
29. Callaghan R, Higgins CF. Interaction of tamoxifen with the multidrug resistance P-glycoprotein. Br J Cancer. 1995; 71:294–9. [PubMed: 7841043]
30. Esposito F, Tornincasa M, Federico A, Chiappetta G, Pierantoni GM, Fusco A. High-mobility group A1 protein inhibits p53-mediated intrinsic apoptosis by interacting with Bcl-2 at mitochondria. Cell Death Dis. 2012; 3:e383. [PubMed: 22932725]
31. Hsu HH, Cheng SF, Wu CC, Chu CH, Weng YJ, Lin CS, et al. Apoptotic effects of over-expressed estrogen receptor-beta on LoVo colon cancer cell is mediated by p53 signalings in a ligand-dependent manner. Chin J Physiol. 2006; 49:110–6. [PubMed: 16830793]
32. Habold C, Poehlmann A, Bajbouj K, Hartig R, Korkmaz KS, Roessner A, et al. Trichostatin A causes p53 to switch oxidative-damaged colorectal cancer cells from cell cycle arrest into apoptosis. J Cell Mol Med. 2008; 12:607–21. [PubMed: 18419600]
33. Tan J, Zhuang L, Leong HS, Iyer NG, Liu ET, Yu Q. Pharmacologic modulation of glycogen synthase kinase-3beta promotes p53-dependent apoptosis through a direct Bax-mediated mitochondrial pathway in colorectal cancer cells. Cancer Res. 2005; 65:9012–20. [PubMed: 16204075]

34. Zolnik BS, Stern ST, Kaiser JM, Heakal Y, Clogston JD, Kester M, et al. Rapid distribution of liposomal short-chain ceramide in vitro and in vivo. Drug Metab Dispos. 2008; 36:1709–15. [PubMed: 18490436]
35. Shen LZ, Hua YB, Yu XM, Xu Q, Chen T, Wang JH, et al. Tamoxifen can reverse multidrug resistance of colorectal carcinoma in vivo. World J Gastroenterol. 2005; 11:1060–4. [PubMed: 15742416]
36. Hotta T, Tanimura H, Yamaue H, Iwahashi M, Tani M, Tsunoda T, et al. Tamoxifen circumvents the multidrug resistance in fresh human gastrointestinal cancer cells. J Surg Res. 1996; 66:31–5. [PubMed: 8954828]
37. Leonessa F, Jacobson M, Boyle B, Lippman J, McGarvey M, Clarke R. Effect of tamoxifen on the multidrug-resistant phenotype in human breast cancer cells: isobologram, drug accumulation, and M(r) 170,000 glycoprotein (gp170) binding studies. Cancer Res. 1994; 54:441–7. [PubMed: 7903910]
38. Nakayama Y, Sakamoto H, Satoh K, Yamamoto T. Tamoxifen and gonadal steroids inhibit colon cancer growth in association with inhibition of thymidylate synthase, survivin and telomerase expression through estrogen receptor beta mediated system. Cancer Lett. 2000; 161:63–71. [PubMed: 11078914]
39. Lindner DJ, Borden EC. Synergistic antitumor effects of a combination of interferon and tamoxifen on estrogen receptor-positive and receptor-negative human tumor cell lines in vivo and in vitro. J Interferon Cytokine Res. 1997; 17:681–93. [PubMed: 9402106]
40. Lointier P, Wildrick DM, Boman BM. Growth effects of tamoxifen on Lovo colon carcinoma cells and cultured cells from normal colonic mucosa. Anticancer Res. 1992; 12:1523–5. [PubMed: 1444215]
41. Nica AF, Tsao CC, Watt JC, Jiffar T, Kurinna S, Jurasz P, et al. Ceramide promotes apoptosis in chronic myelogenous leukemia-derived K562 cells by a mechanism involving caspase-8 and JNK. Cell Cycle. 2008; 7:3362–70. [PubMed: 18948750]
42. Furlong SJ, Ridgway ND, Hoskin DW. Modulation of ceramide metabolism in T-leukemia cell lines potentiates apoptosis induced by the cationic antimicrobial peptide bovine lactoferricin. Int J Oncol. 2008; 32:537–44. [PubMed: 18292930]
43. Gutierrez G, Mendoza C, Montano LF, Lopez-Marure R. Ceramide induces early and late apoptosis in human papilloma virus+ cervical cancer cells by inhibiting reactive oxygen species decay, diminishing the intracellular concentration of glutathione and increasing nuclear factor-kappaB translocation. Anticancer Drugs. 2007; 18:149–59. [PubMed: 17159601]
44. Takeda S, Mitsutake S, Tsuji K, Igarashi Y. Apoptosis occurs via the ceramide recycling pathway in human HaCaT keratinocytes. J Biochem. 2006; 139:255–62. [PubMed: 16452313]
45. Stover T, Kester M. Liposomal delivery enhances short-chain ceramide-induced apoptosis of breast cancer cells. J Pharmacol Exp Ther. 2003; 307:468–75. [PubMed: 12975495]
46. Stover TC, Sharma A, Robertson GP, Kester M. Systemic delivery of liposomal short-chain ceramide limits solid tumor growth in murine models of breast adenocarcinoma. Clin Cancer Res. 2005; 11:3465–74. [PubMed: 15867249]
47. Liu X, Ryland L, Yang J, Liao A, Aliaga C, Watts R, et al. Targeting of survivin by nanoliposomal ceramide induces complete remission in a rat model of NK-LGL leukemia. Blood. 2010; 116:4192–201. [PubMed: 20671121]

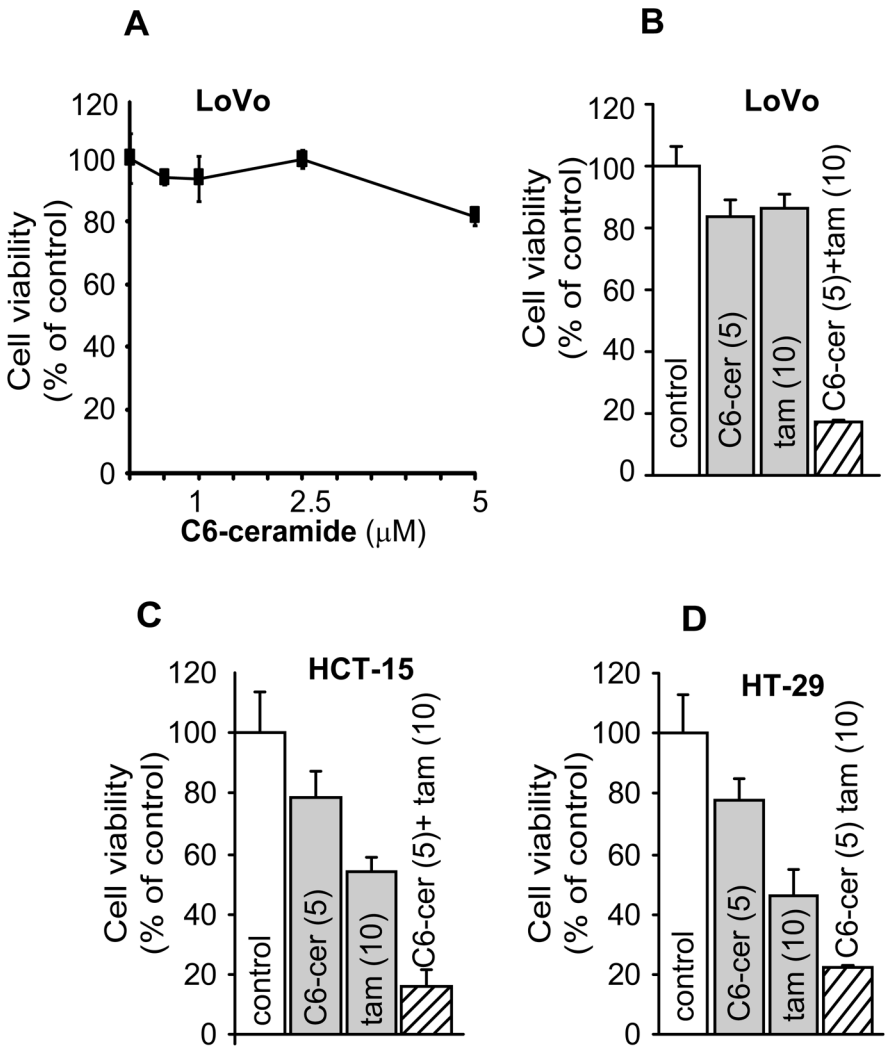

Fig. 1.

Effect of C6-ceramide and tamoxifen on colorectal cancer cell viability. (A) C6-ceramide dose-response in LoVo cells. (B–D) Effect of single agent and combination treatments. Cells were seeded in 96-well plates and treated the following day as shown; concentrations (μM) noted in parentheses. Viability was assessed after 72 h exposure using Promega MTS reagent. n=6 per experimental group; values are the mean ± S.E. Drug combinations are statistically significant ($P \leq 0.05$) compared to control and single agents. Repeated experiments yielded similar results. C6-cer, C6-ceramide; tam, tamoxifen.

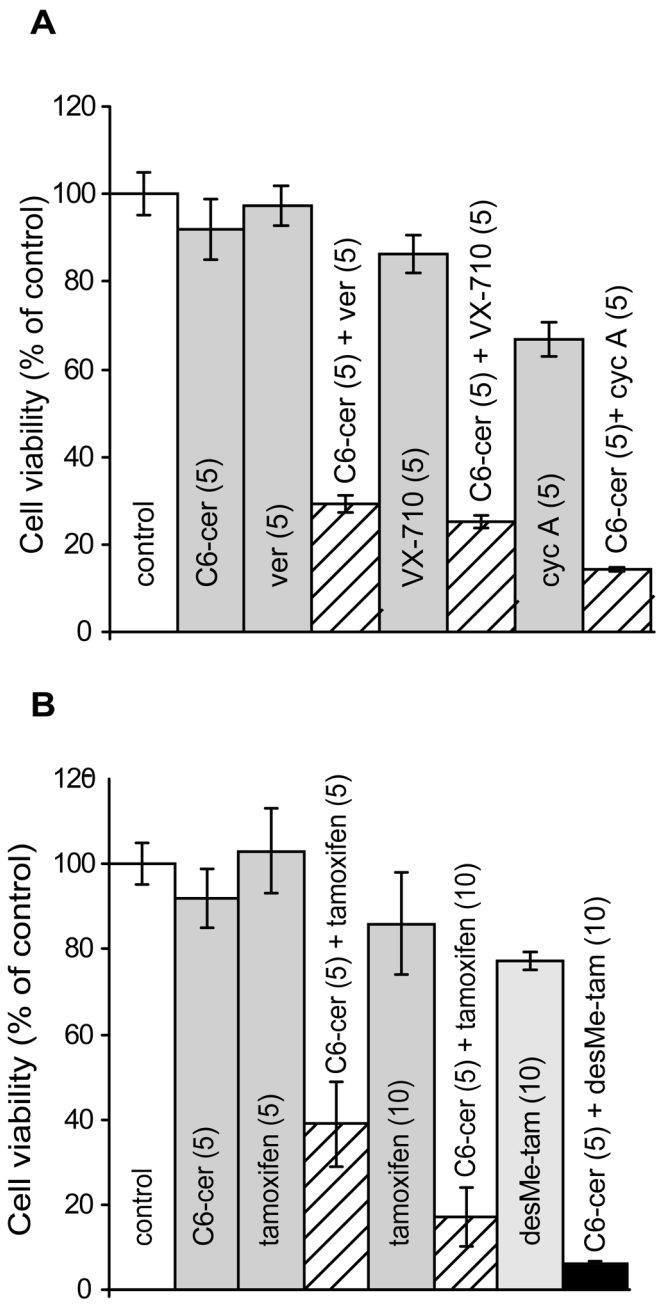

Fig. 2.

Effect of conventional P-gp antagonists, tamoxifen, and the tamoxifen metabolite *N*-desmethyltamoxifen on C6-ceramide cytotoxicity in LoVo cells. (A) Effect of Verapamil, VX-710, and cyclosporin A on C6-ceramide cytotoxicity. (B) Effect of tamoxifen and *N*-desmethyltamoxifen on C6-ceramide cytotoxicity. LoVo cells were seeded in 96-well plates and treated the following day as indicated; concentrations (μM) noted in parentheses. Ethanol was the vehicle for all agents. Viability was measured after 72 h. n=6 per experimental group; values are the mean ± S.E. Drug combinations are statistically significant ($P \leq 0.05$) compared to control and single agents. C6-cer, C6-ceramide; ver, verapamil; cyc A; cyclosporin A; desMe-tam, *N*-desmethyltamoxifen.

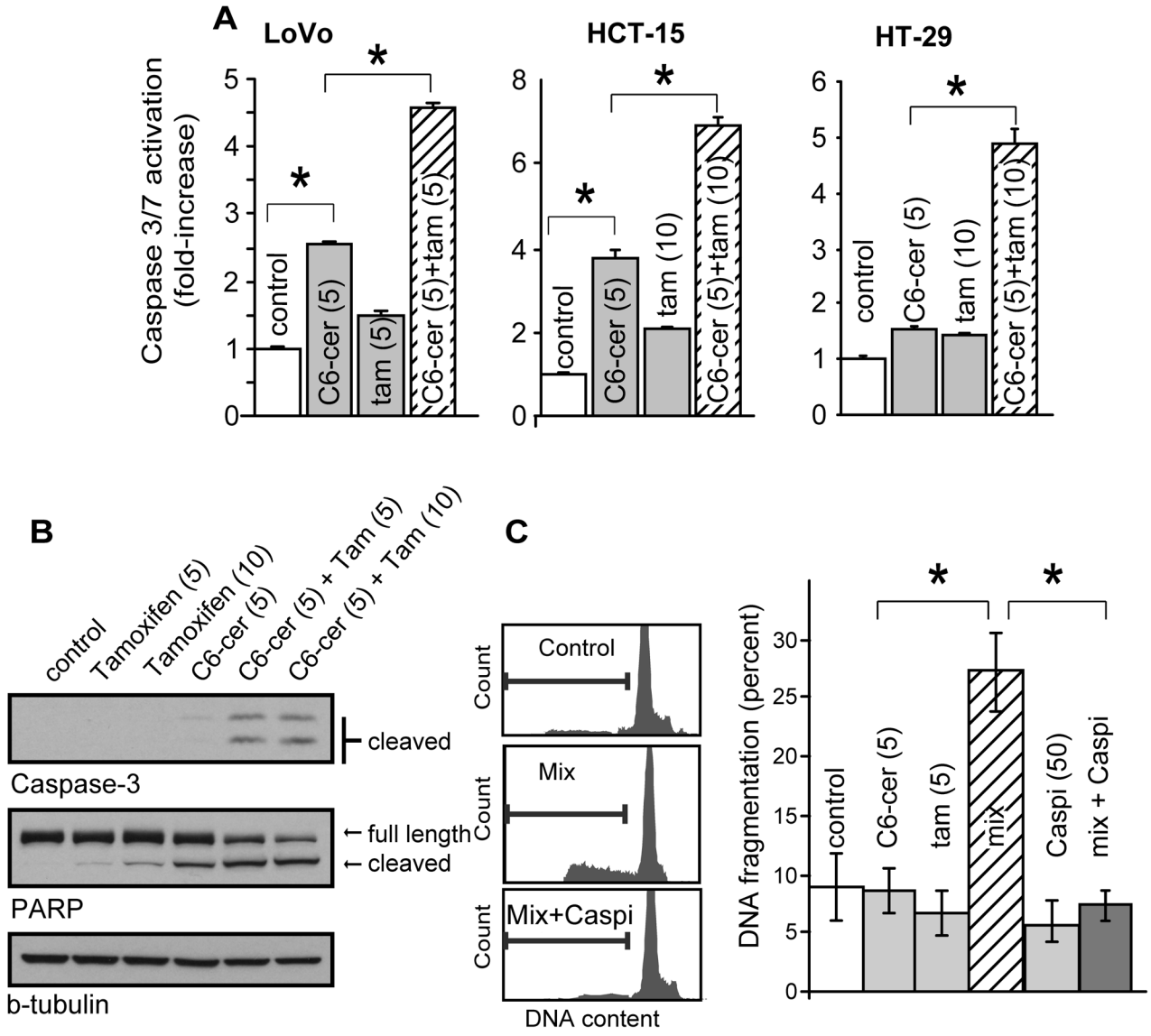

Fig. 3.

Effect of C6-ceramide and tamoxifen on caspase activation, PARP cleavage, and DNA fragmentation, in LoVo cells. (A) Caspase-3/7 activation. Cells were seeded in 96-well plates and treated the following day as indicated. Caspase-3/7 activation was determined after 24 h exposure, using a Promega kit, as described. (B) Caspase-3 activation and PARP cleavage. Cells (500,000) were seeded in 6-cm dishes 24 h prior to 24 h treatment as indicated. Activities were determined by Western blot as detailed in Methods. (C) DNA fragmentation. Cells (200,000/6-cm dish) were seeded in 10% FBS medium and treated the following day, as indicated, in medium containing 2.5% FBS, for 24 h. DNA was stained and content analyzed by flow cytometry as detailed in Methods. (C) Left panel, flow cytometry read-out; right panel, quantitation by bar graph. Concentrations (μM) noted in parentheses. Caspi, pan-caspase inhibitor Z-VAD-FMK. *, $P \leq 0.05$.

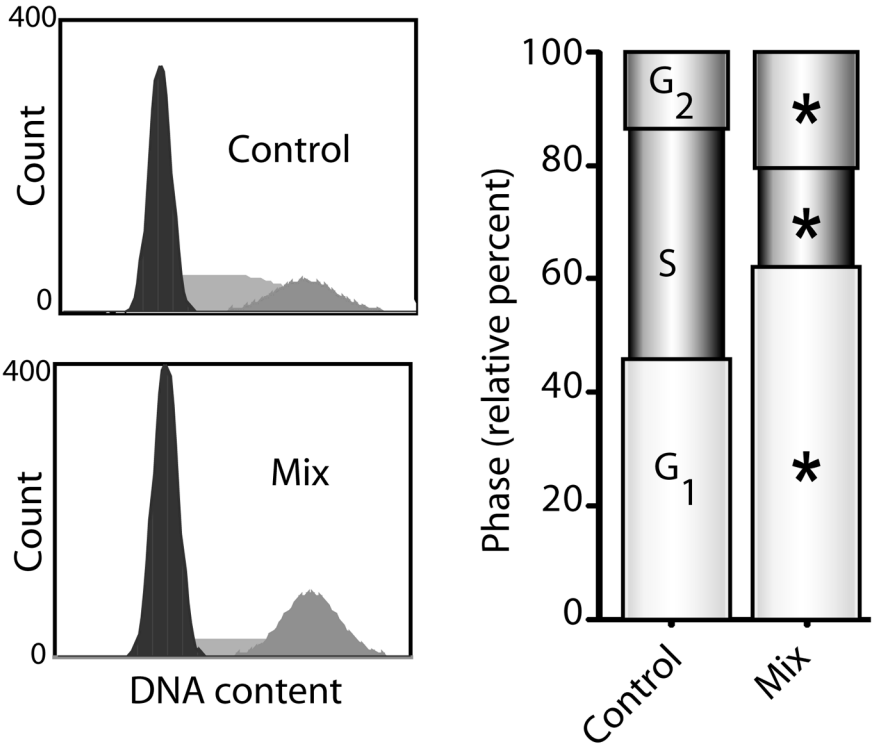

Fig. 4.

Effect of C6-ceramide-tamoxifen on LoVo cell cycle traverse. Cells (200,000/6-cm dish) were seeded and treated after 24 h with C6-ceramide-tamoxifen, each at 5 μM, for 24 h. Analyses were performed using FCS express 4 (De Novo Software). Left panel, flow cytometry analysis of DNA content; right panel, cell cycle phase quantitation. Mix, C6-ceramide-tamoxifen. *, $P \leq 0.05$.

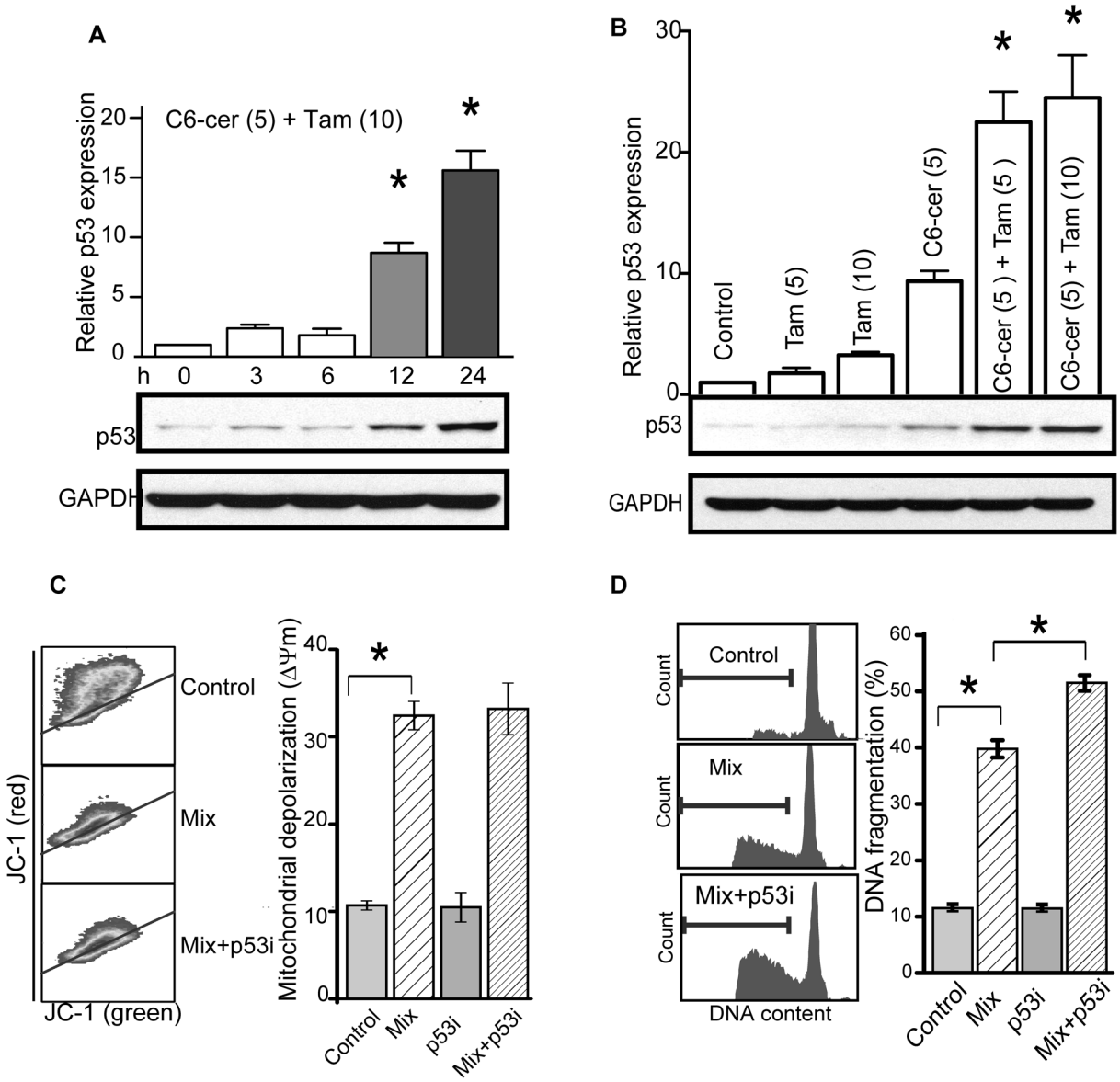

Fig. 5.

Effect of C6-ceramide and tamoxifen on p53 expression, and the effect of p53 inactivator on C6-ceramide-tamoxifen-induced mitochondrial depolarization and DNA fragmentation in LoVo cells. (A) Effect of exposure time on p53 expression. Treatment consisted of the mixed drug regimen. (B) Effect of single agents and combination treatment on p53 expression. Cells (500,000/6-cm dish) were seeded 24 h prior to treatment. At the times indicated (A), or after 24 h (B), cell lysates (40 μg protein) were resolved by SDS-PAGE and probed with antibody as detailed in Methods. Quantitation was by densitometry. Concentrations (μM) noted in parenthesis. (C) MMP response and the effect of p53 inhibitor. (D) DNA fragmentation and effect of p53 inhibitor. Cells were seeded as above and treated as shown, and MMP and DNA fragmentation were measured as described in Methods. Triplicate cultures were used for all experimental conditions, and data are the mean ± S.E. Mix, C6-ceramide-tamoxifen combination; p53i, p53 inactivator (Pifithrin-α) (10 μM). (C–D) C6-ceramide, 5 μM; tamoxifen, 10 μM. *, $P \leq 0.05$.

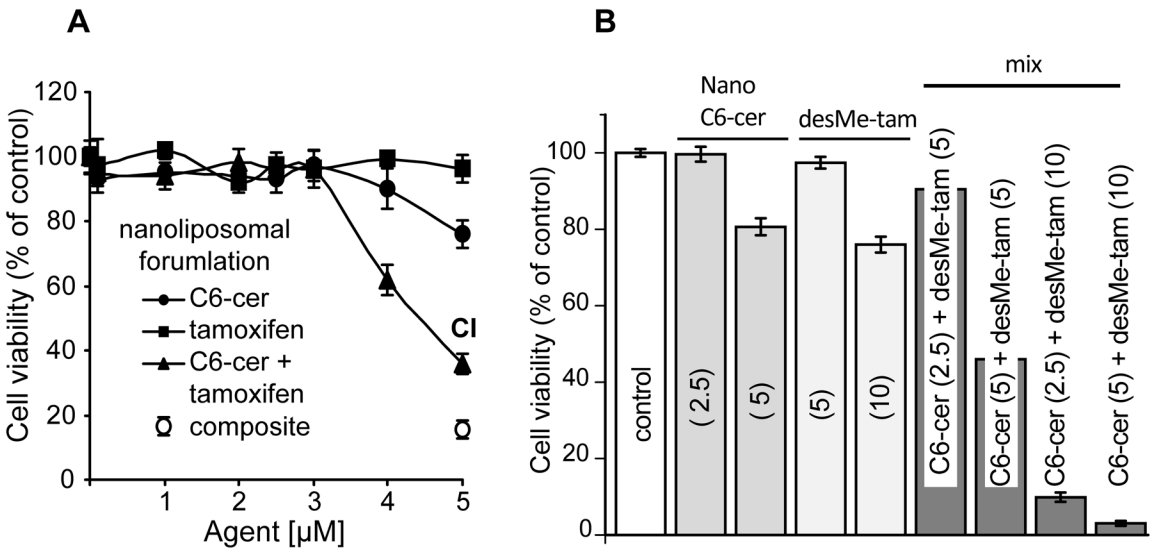

Fig. 6.

Effect of nanoliposomal formulations of C6-ceramide, tamoxifen, and *N*-desmethyltamoxifen on LoVo cell viability. (A) Effect of nanoliposomal formulations. Cells, seeded in 96-well plates, were exposed the following day to the nano-formulated agents shown, at increasing concentrations. Viability was determined after 72 h exposure. CI denotes combination index, which was 0.37. Nanoliposomes were formulated as described in Methods. Composite nanoliposomes contained both C6-ceramide and tamoxifen in the same particle. n=6 per experimental group; values are the mean ± S.E. (B) Effect of nanoliposomal C6-ceramide and *N*-desmethyltamoxifen (desMe-tam) (ethanol vehicle) on LoVo cell viability. Cell seeding and exposure time, as in A. n=6 per experimental group; values are the mean ± S.E. Drug combination effects are statistically significant ($P \leq 0.05$) compared to control and single agents. Concentrations (μM) noted in parenthesis.

Table 1

Effect of tamoxifen on metabolism of C6-ceramide in LoVo cells

Additions	Sphingolipids (% of total ^{14}C)			
	C6-cer	C6-GC	C6-LC	C6-SM
− tamoxifen	10.43 ± 0.8	82.3 ± 1.1	0.96 ± 0.07	6.31 ± 0.26
+ tamoxifen	23.1 ± 1.73*	58.87 ± 1.15*	1.4 ± 0.35	16.63 ± 0.25*

Cells were pretreated with tamoxifen (5.0 μM) 1 h before addition of [^{14}C]C6-ceramide (20 μM) for 24 h. This concentration of C6-ceramide was not cytotoxic at 24 h. Total cellular lipids were extracted and analyzed by TLC and LSC as detailed in Methods. Percentages of each lipid class were calculated from the total lipid ^{14}C dpm. Results represent the average of triplicate cultures ± S.E. C6-cer, C6-ceramide; GC, glucosylceramide; LC, lactosylceramide; SM, sphingomyelin.

*$P \leq 0.05$, Student's t Test.